THE JOURNAL OF PHYSICAL CHEMISTRY C

Article

Cite This: J. Phys. Chem. C XXXX, XXX, XXX−XXX

pubs.acs.org/JPCC

# High Remaining Factors in the Photovoltaic Performance of Perovskite Solar Cells after High-Fluence Electron Beam Irradiations

Zhaoning Song,*[,†] Chongwen Li,[†] Cong Chen,[†] Jeremiah McNatt,[‡] Woojun Yoon,[§] David Scheiman,[§] Phillip P. Jenkins,[§] Randy J. Ellingson,[†] Michael J. Heben,[†] and Yanfa Yan*[,†]

[†]Department of Physics and Astronomy, Wright Center for Photovoltaics Innovation and Commercialization, University of Toledo, 2801 W. Bancroft Street, Toledo, Ohio 43606, United States

[‡]NASA Glenn Research Center, 21000 Brookpark Rd, Cleveland, Ohio 44135, United States

[§]Naval Research Laboratory, 4555 Overlook Avenue S.W., Washington, DC 20375, United States



**ABSTRACT:** Metal halide perovskite solar cells have progressed rapidly over the past decade, providing an exceptional opportunity for space photovoltaic (PV) power applications. However, the solar cells to be used for space power have to demonstrate a stable operation under extreme conditions, particularly concerning harsh radiations. In contrast to previously reported superior stability of low PV performance perovskite solar cells against high-energy radiation, we investigate the effects of high-energy electron beam irradiation on the degradation of perovskite solar cells with a high-power conversion efficiency exceeding 20%. We find very high remaining factors of >87.7% in the open-circuit voltage ($V_{OC}$) and >93.5% in the fill factor (FF) and a significantly decreased short-circuit current density ($J_{SC}$) after the exposure to high-fluence electron irradiations of $10^{15}$ e/cm$^2$. The pronounced loss of $J_{SC}$ is due to the decreasing transmittance of the soda-lime glass substrate and the partial decomposition of the perovskite absorber layers. The irradiated cells retained superior remaining factors in both $V_{OC}$ and FF, demonstrating a superior tolerance of perovskite solar cells after the exposure to the electron irradiation. These results show that perovskite solar cells hold great potential for space PV power applications if stable perovskite compositions and space-suitable substrates are employed.

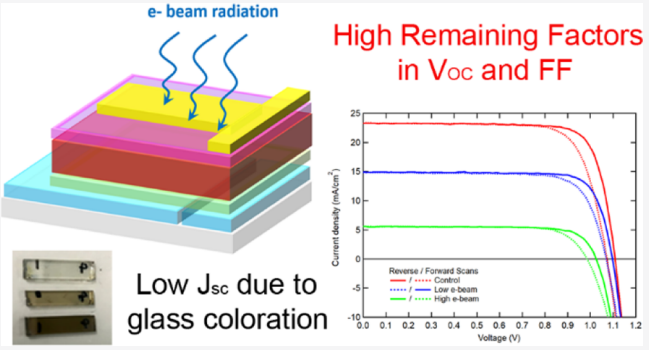


## INTRODUCTION

The past decade has witnessed an impressive development of solar cells based on metal halide perovskites at an unprecedented speed. The solar-to-electricity power conversion efficiency (PCE) of perovskite solar cells (PSCs) has increased rapidly from less than 4% to more than 25%,[1,2] which rivals other more established photovoltaic (PV) technologies. Additionally, PSCs possess some manufacturing advantages,[3] including low material and processing costs[4] and low-temperature deposition approaches that enable the use of flexible and lightweight substrates for high specific weight power applications like portable power sources and unmanned aerial vehicles.[5−7] The advances in PSCs provide an exceptional opportunity for the fabrication of low-cost, high-efficiency, lightweight solar cells for space power applications.[8] However, as a reliable power source, solar cells to be used for space power have to tolerate high-energy cosmic radiation, including protons, electrons, and $\gamma$-rays.[9] Although PSCs are promising to be used for space power applications because of their noteworthy performance, their stability under cosmic radiation is yet be demonstrated.

To date, a few experiments have been carried out to examine the tolerance of PSCs under the influence of proton,[10−13] electron,[11−13] neutron,[14] and $\gamma$-ray irradiations[15,16] and in an on-field test in near space.[17] Lang et al. investigated the impacts of proton irradiation on $MAPbI_3$ PSCs with initial PCEs of ∼12%,[10] revealing radiation hardness and self-healing in PSCs. Further analysis showed that proton irradiation improved the recombination lifetime of photogenerated charge carriers in the perovskites.[18] Miyazawa et al. irradiated high-energy electron and proton beams on PSCs in a simulated space environment.[11] The poly(3-hexylthiophene)-based solar cells with PCEs less than 9% demonstrated a sufficiently high durability against high-fluence irradiations of up to $10^{16}$ particles/cm$^2$. Huang et al. examined the effects of electron and proton irradiations on PSCs with initial PCEs of ∼12%, showing only a slight degradation in PV performance.[12] Yang et al. investigated the stability of perovskites under $\gamma$-ray radiation and concluded that perovskites are more robust than glass under $\gamma$-rays.[15] Although these reports demonstrated robust radiation hardness of PSCs, most studies employed

Received: December 11, 2019
Revised: December 19, 2019
Published: December 20, 2019




DOI: 10.1021/acs.jpcc.9b11483
J. Phys. Chem. C XXXX, XXX, XXX−XXX

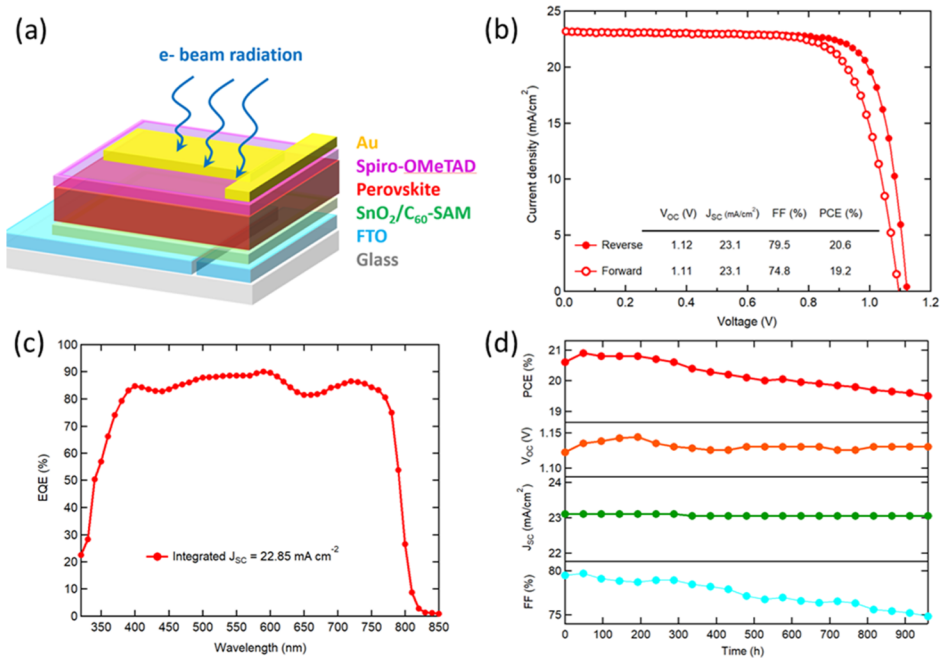


**Figure 1.** (a) Schematic of a PSC used for the radiation test. (b) $J-V$ and (c) EQE of a typical pristine PSC. (d) PV parameter evolution as a function of storage time in a nitrogen glovebox.

PSCs with relatively low or moderate PCEs, which make these promising results less convincing and speculative.

In contrast to the positive outcomes of radiation tolerance, it has also been reported that high-energy radiation can deteriorate PSCs. Yang et al. and Boldyreva et al. individually reported that PSCs experienced obvious performance degradation under $\gamma$-ray irradiation.[16,19] In a real field test to assess PSCs for space solar power applications,[20] researchers showed almost 36% power loss after a balloon flight in the stratosphere. Additionally, the perovskite material and device degradation induced by electron beam (e-beam) irradiation has been widely studied using electron microscope-based techniques.[21−24] Despite a much lower electron energy range (keV for electron microscopic measurement vs MeV for space solar stability test), significant material and device degradation was identified after a high dose of e-beam irradiation. The controversial results of the robustness of PSCs against high-energy irradiation show the necessity to have more studies on the radiation tolerance of high-performance PSCs to better evaluate the feasibility of PSCs for future aerospace applications. Moreover, further investigations are needed toward a better understanding of radiation-induced degradation and damage mechanisms in PSCs.

Notably, it is required for the use of electron irradiations in the standard space solar cell qualification test to predict the degradation of solar cells in space.[25] So far, little work has been done with the focus on evaluating the stability of PSCs under e-beam irradiation,[11−13] and all the PSCs used for previous e-beam tolerance studies exhibited moderate or low PCEs of 4−13%. Here, we study the impact of high-fluence e-beam irradiations on the device performance of high-performance PSCs with PCE exceeding 20%. To investigate the e-beam radiation hardness of PSCs, we track the evolution of PV characteristics of PSCs after exposure to 1 MeV e-beam to an accumulated fluence of $10^{13}$ and $10^{15}$ e/cm$^2$ and characterize the changes in materials and devices induced by the e-beam irradiations to study radiation-induced defect generation.

## EXPERIMENTAL METHODS

The PSCs were fabricated on fluorine-doped tin oxide (FTO)-coated glass substrates with a sheet resistance of 15 Ω/sq. The glass/FTO substrates were laser-patterned and cleaned before use. A $SnO_2$ electron transport layer was deposited by plasma-enhanced atomic layer deposition and treated with water vapor.[26] A self-assembled fullerene monolayer ($C_{60}$-SAM) was deposited on $SnO_2$ by spin-coating using a previously reported recipe.[27] The perovskite precursor solution was prepared by dissolving 461 mg $PbI_2$ (TCI), 111 mg methylammonium iodide (MAI, Greatcell Solar), 52 mg formamidinium iodide (FAI, Greatcell Solar), and 9.2 mg $Pb(SCN)_2$ (Sigma) in a mixed solvent of dimethylformamide and dimethyl sulfoxide (DMF/DMSO v/v = 9:1). The perovskite precursor solution was spin-coated on the substrate at 500 rpm for 3 s and then at 4000 rpm for 60 s. A 700 $\mu$L of diethyl ether was dropped on the spinning substrate at 10 s of the second spin step. After spin-coating, the perovskite films were annealed on a hot plate at 65 °C for 2 min and 100 °C for 2 min. After this, a spiro-OMeTAD solution was prepared and spin-coated on the perovskite layers, as reported previously.[28] Finally, devices were completed by depositing an 80 nm Au layer using thermal evaporation. The devices were then patterned into an active area of ∼0.8 cm$^2$ using laser scribing.

$J-V$ and steady-state efficiency curves were recorded using a Keithley 2400 source meter under standard 100 mW/cm$^2$ illumination (AM 1.5G) using a PV Measurements solar simulator. External quantum efficiency (EQE) curves in the range of 300−850 nm were measured using a PV Measurements EQE system calibrated with a certified Si photodiode. The optical transmittance spectra in the range of 300−850 nm were obtained using a PerkinElmer Lambda 1050 spectrometer. Cross-sectional scanning electron microscopy (SEM) and energy-dispersive X-ray spectroscopy (EDX) microanalysis on PSCs were performed using a Hitachi S-4800 field emission electron microscope. X-ray diffraction (XRD) spectra in the


DOI: 10.1021/acs.jpcc.9b11483
J. Phys. Chem. C XXXX, XXX, XXX−XXX

range of 10−18° were measured with a step size of 0.02° at a speed of 0.1° per min using a Rigaku Ultima III X-ray diffractometer. Laser beam-induced current (LBIC) maps of PSCs were obtained using a built-in-house multifunction laser system.[29]

To test the tolerance of PSCs to e-beam irradiation, pristine perovskite cells were fabricated at Toledo and shipped to the NEO Beam facility at NASA Glenn Research Center. Sixteen identical unencapsulated cells were loaded on the irradiation plate and exposed to 1 MeV e-beam irradiation. After a fluence of $1.3 \times 10^{13}$ e/cm$^2$ irradiation (denoted by low e-beam), half of the devices were removed. The remaining cells were removed after an accumulated fluence of $1 \times 10^{15}$ e/cm$^2$ irradiation (denoted by high e-beam). The maximum temperature of ∼50 °C can be reached under the NEO beam irradiation. To compare with the e-beam-irradiated devices, eight control devices traveled with the irradiated cells to the exposure area, remained in the same general environmental condition as the irradiated cells (open warehouse environment, ambient humidity, and temperature), returned with the irradiated cells, and sealed in a vacuum bag after exposure.

## RESULTS AND DISCUSSION

Figure 1a shows the schematic sketch of the device structure of the PSCs used in this study. The devices in the so-called n−i−p configuration were constructed by sequentially depositing a thin-film stack, including atomic layer-deposited $SnO_2$, spin-coated fullerene self-assembled monolayer ($C_{60}$-SAM), $MA_{0.7}FA_{0.3}PbI_3$ perovskite absorber layer (where MA and FA are methylammonium and formamidinium), and 2,2′,7,7′-tetrakis(*N*,*N*-di-*p*-methoxyphenylamine)-9,9′-spirobifluorene (spiro-OMeTAD), and a thermally evaporated Au electrode on laser-patterned FTO-coated soda-lime glass substrates, following the fabrication process reported previously.[26,28,30] Experimental details on device fabrication are provided in the Experimental Methods section. The device fabrication is based on a well-established recipe that can be used to fabricate more than 20% efficient PSCs. Figure 1b shows the current density−voltage ($J$−$V$) curves of a typical device under 100 mW/cm$^2$ simulated standard solar illumination (AM 1.5G). The device delivers a PCE of 20.6 (19.2)%, with an open-circuit voltage ($V_{OC}$) of 1.12 (1.11) V, a short-circuit current density ($J_{SC}$) of 23.1 (23.1) mA/cm$^2$, and a fill factor (FF) of 79.5 (74.8)% when measured under a reverse (forward) voltage scan. It is worth noting that such a small degree of $J$−$V$ hysteresis is typically observed in PSCs.[31] The external quantum efficiency (EQE) curve of the device is shown in Figure 1c. The integrated photocurrent density is 22.85 mA/cm$^2$, which is within 1% deviation from the $J_{SC}$ value determined by the $J$−$V$ measurement. The shelf stability of an unencapsulated device stored in the nitrogen environment is demonstrated in Figure 1d. The PCE of the device decreased from 20.6 to 19.5% after storage for 960 h (40 days), accounting for a relative efficiency drop of 5%. As a remark, the storage degradation is mainly caused by decreasing FF, likely because of degassing of oxygen from spiro-OMeTAD that lowers the hole mobility,[32] whereas the $V_{OC}$ and $J_{SC}$ values almost remained the same during the storage period. Because of high performance and adequate stability, devices in this configuration were selected for the test of e-beam radiation hardness.

Figure 2 shows the statistical distribution of PV parameters for devices under control and under low and high e-beam irradiation conditions. The average PCEs of irradiated cells

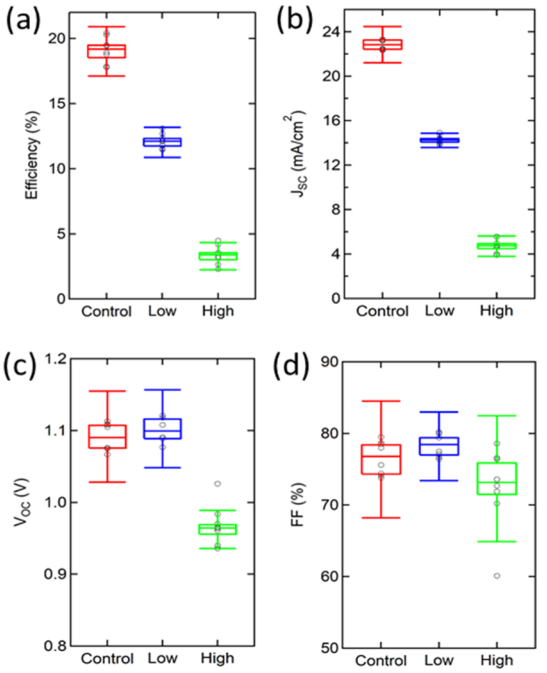


**Figure 2.** Distributions of PV parameters, including (a) efficiency, (b) $J_{SC}$, (c) $V_{OC}$, and (d) FF for 12 PSCs under control and low and high e-beam irradiation conditions.

under the low and high fluence of e-beam decreased to 12.2 and 3.4%, respectively, corresponding to 36 and 82% drops compared with the average PCE of 19.2% for the control devices (Figure 2a). The primary cause for the efficiency drop is attributed to the pronounced decrease in $J_{SC}$ values (Figure 2b), corresponding to the $J_{SC}$ drops of 8.4 and 18.1 mA/cm$^2$ for the low and high e-beam-irradiated devices, respectively, when compared with the control devices. Interestingly, the impacts of e-beam irradiation on $V_{OC}$ and FF are much less significant (Figure 2c,d), showing very high remaining factors (Table 1). The low e-beam irradiation even leads to slight increases in $V_{OC}$ and FF, whereas the high fluence irradiation indeed deteriorates the $V_{OC}$ and FF values. Overall, the results agree with Miyazawa et al.,[11] who reported high radiation tolerance of PSCs under e-beam irradiation at $10^{16}$ e/cm$^2$. The discrepancy may be related to the device configuration or initial performance (20 vs 5%). The relatively low initial PCEs could make it hard to distinguish the subtle changes in the device performance.

Figure 3a presents the $J$−$V$ curves of representative control and irradiated cells under forward and reverse voltage scans. The degradation of irradiated perovskite cells is mainly attributed to the significantly decreased photocurrent density. The $J$−$V$ curves of irradiated cells remain in good shape, indicating that the e-beam irradiation has an insignificant impact on the diode behavior of the cells to rectify current. Despite decreased PCEs, the irradiated devices exhibit stabilized power output as the control cell under 1 sun illumination, as shown in Figure 3b. These results indicate that the high-energy electron irradiation does not significantly affect other layers in the PSCs, such as the charge-selective layers ($SnO_2$/$C_{60}$ and spiro-OMeTAD) and electrodes (FTO and Au). The EQE measurement (Figure 3c) reveals that the irradiated cells exhibit significant drops in spectrally dependent photocurrent response compared with the control device, especially in the short wavelength range (350−650 nm). The


DOI: 10.1021/acs.jpcc.9b11483
J. Phys. Chem. C XXXX, XXX, XXX−XXX

**Table 1. Remaining Factors in the PV Parameters of Control and Irradiated PSCs**

| | | remaining factor | | | |
|---|---|---|---|---|---|
| | scan direction | $V_{OC}$ (%) | FF (%) | $J_{SC}$ (%) | PCE (%) |
| control | reverse | 99.8 ± 0.4 | 101.3 ± 0.4 | 100.3 ± 2.0 | 101.5 ± 2.6 |
| | forward | 100.2 ± 0.5 | 103.8 ± 0.7 | 100.9 ± 2.4 | 105.2 ± 3.9 |
| 1 MeV e-beam irradiation with a fluence of $1.3 \times 10^{13}$ e/cm | reverse | 98.3 ± 0.4 | 101.6 ± 0.3 | 81.3 ± 1.4[a] | 81.0 ± 1.6[b] |
| | forward | 98.6 ± 0.4 | 103.9 ± 0.4 | 80.7 ± 1.3[a] | 82.6 ± 1.0[b] |
| 1 MeV e-beam irradiation with a fluence of $1.3 \times 10^{15}$ e/cm | reverse | 87.7 ± 2.7 | 93.5 ± 4.2 | 68.4 ± 3.1[a] | 56.3 ± 6.6[b] |
| | forward | 89.3 ± 1.9 | 96.2 ± 10.8 | 68.3 ± 2.9[a] | 59.0 ± 9.6[b] |

[a]The remaining factors in $J_{SC}$ are corrected to consider the loss in the transmittance of the glass substrate. [b]The values of PCE are corrected accordingly using the corrected $J_{SC}$, and PCE is measured under a simulated AM 1.5G spectrum (100 mW/cm$^2$).

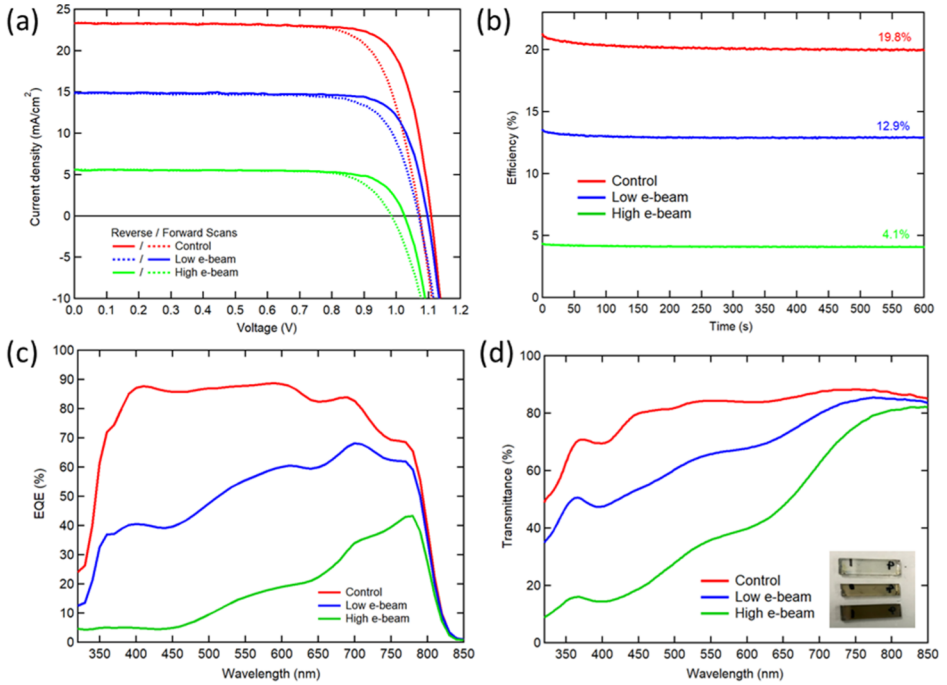


**Figure 3.** (a) $J$–$V$, (b) steady-state efficiency, and (c) EQE of PSCs under control, low e-beam, and high e-beam conditions. (d) Optical transmittance of FTO glass substrates before and after e-beam radiation. Inset of panel (d) is a photo of glass debris from the tested cells after cleaning.

optical transmittance measurement was conducted on the cleaned glass substrates after removing the thin film stacks of PSCs from the tested devices. After receiving a high fluence of e-beam irradiation, the color of the glass substrate became darker, as shown in the inset of Figure 3d. The optical transmittance spectra (Figure 3d) confirm the loss of transparency at the short wavelengths, consistent with the pronounced drops in the EQE spectra. The loss of optical transparency because of the creation of color centers in the glass substrate is in good agreement with the previous reports of PSCs under high-energy protons[10] and $\gamma$-ray photons.[16] It has also been shown that the energetic proton beam can cause increased optical absorption in common thin-film PV substrates such as soda-lime glass and polyethylene terephthalate foils.[33] To overcome the shading effect, space solar cover glass typically incorporates lanthanum or cerium to enhance its radiation hardness.[34] Alternatively, quartz substrates can resist proton and e-beam radiation well.[11] Taking into account the optical loss in the glass substrates, we would expect the loss in $J_{SC}$ by 4.0 and 10.7 mA/cm$^2$, resulting in decent remaining factors of 63.3 ± 1.4 and 68.4 ± 2.8%, respectively, for low and high e-beam-irradiated devices. Although these values are much less than the measured $J_{SC}$ degradation of 8.4 and 18.1 mA/cm$^2$, we expect that the e-beam induced damages to the perovskite absorber layers to some degree.

Material and device analyses were then conducted to evaluate the degradation of the perovskite absorber layers because of e-beam irradiation. Figure 4a–c shows the cross-sectional SEM images of the control and irradiated PSCs. No clear visual damage has been found in the microscopic structure of the devices. All the thin-film layers were preserved after the exposure to a high fluence of e-beam irradiation. However, the EDX measurement reveals that the molar ratio of Pb to I was changed from 1:2.9 for the control to 1: 2.5 and 1:2.2 for the low and high e-beam-irradiated samples (Figure 4d–f), respectively, indicating the partial decomposition of perovskite (Pb/I = 1:3) into the photoinactive lead iodide (Pb/I = 1:2). It is worth noting that the organic–inorganic lead halide perovskites are prone to degradation when exposed to humid air,[35,36] heating,[37,38] UV light,[39] electric fields,[40] electron beam,[23] and so forth. During the e-beam irradiation test, the unencapsulated PSCs experienced certain thermal stress because of the e-beam bombardment. The combination


DOI: 10.1021/acs.jpcc.9b11483
J. Phys. Chem. C XXXX, XXX, XXX–XXX

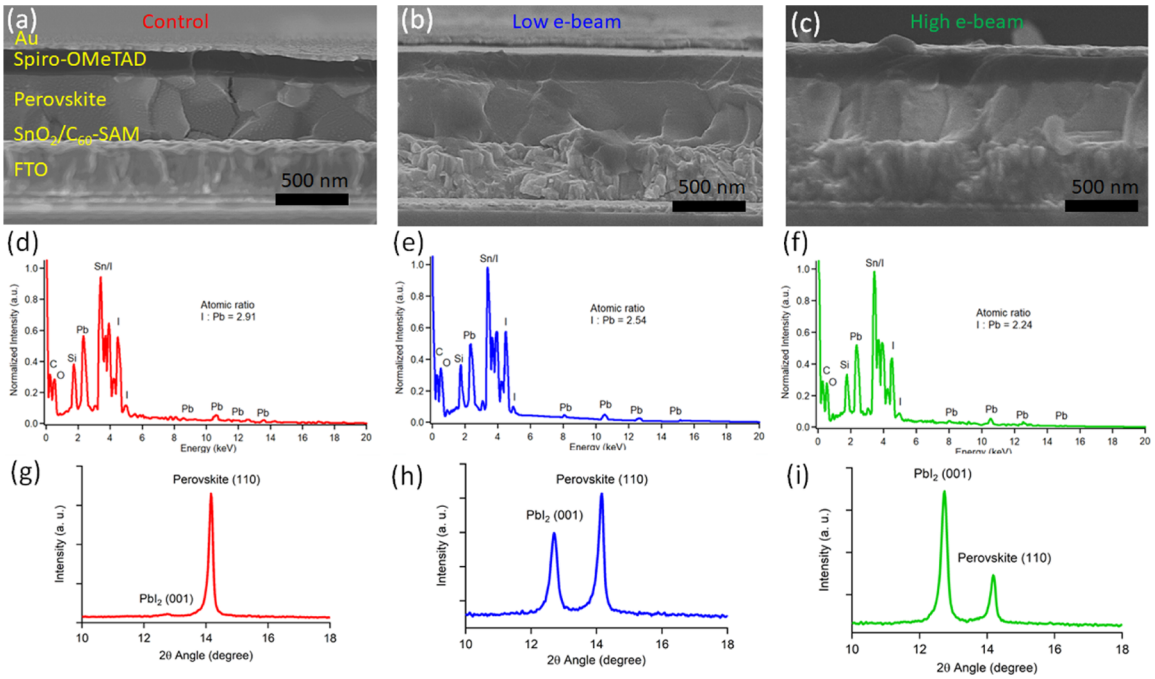


**Figure 4.** Cross-sectional (a–c) SEM images and (d–f) EDX and (g–i) XRD spectra of PSCs under (a,d,g) control, (b,e,h) low e-beam, and (c,f,i) high e-beam conditions.

of elevated temperatures and ambient humidity led to the considerable decomposition of perovskites. The XRD measurement revealed that the hexagonal $PbI_2$ peak at 12.1° increases, whereas the peak of perovskite at 14.1° decreases with increasing e-beam exposure, as shown in Figure 4g–i, confirming the appearance of $PbI_2$ after e-beam irradiation. The partial decomposition of organic–inorganic perovskites accounts for the part of the loss of $J_{SC}$ in addition to primary loss because of the reduced transparency of the glass substrates. Despite the identification of primary causes for the loss of current, the origins of the performance degradation may also be related to the deterioration of doped spiro-OMeTAD or the degradation of the quality of its interface with the perovskite absorber layer, triggered by e-beam-induced heating in a humid ambient. However, a radiation test under a well-controlled environment to evaluate individual influencing factors is beyond the capability of the current study and will be the focus of our follow-up work.

We further probed the spatially resolved photocurrent generation in the devices using the LBIC technique.[35] Figure 5 shows the photocurrent maps of the control and low and high e-beam-irradiated cells. The photocurrent reduction because of e-beam irradiations is resolved by the LBIC mapping. Furthermore, the e-beam damages on the circumferences of the cell close to the edges of the metal back-contact are observed, indicating that the metal back-contact coverage may slightly retard the decomposition of the perovskite by blocking the pathways for the release of volatile decomposition products (e.g., hydrogen iodide and methylamine), which alleviates the e-beam damages on the perovskite layers. Additionally, it is worth noticing that e-beam leads to a homogeneous degradation across the entire device area, which differs from the inhomogeneous degradation because of water ingress.[35] The degradation in the perovskite absorber layer is likely related to the instability of the organic–inorganic metal halide composition, which tends to degrade under illumination

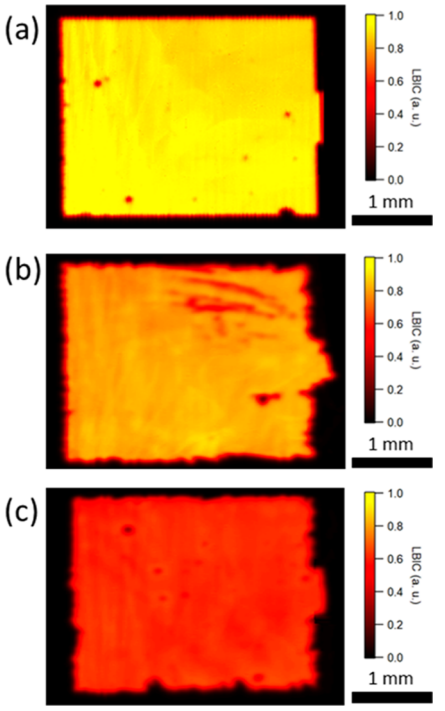


**Figure 5.** LBIC maps of PSCs under (a) control, (b) low e-beam, and (c) high e-beam conditions.

and heat.[37,39,41] Perovskite materials with enhanced thermal stability and photostability (e.g., cesium-based all-inorganic perovskites) and more stable hole-transporting layers are needed for space power applications.[42,43] Recent advances in fabricating high-efficiency (>18%) all-inorganic PSCs[44] show a great promise for investigating the irradiation tolerance of PSCs using more thermodynamically stable perovskite compositions. Moreover, space-qualified substrate and encapsulation are required to ensure the integrity of the perovskite


DOI: 10.1021/acs.jpcc.9b11483
J. Phys. Chem. C XXXX, XXX, XXX–XXX

layer and the complete device to cover the lifetime of desired space applications. Clearly, more investigations are needed in the future to continue the evaluation of the cosmic irradiation stability of PSCs with better intrinsic absorber stability and substrates that can resist irradiations well.

## CONCLUSIONS

In summary, we investigated the impacts of high-fluence e-beam irradiations on the performance of high-efficiency PSCs. We observed very high remaining factors in both $V_{OC}$ and FF but a decent remaining factor in $J_{SC}$ and, consequently, in the PCE of PSCs after e-beam irradiation. Further characterization reveals that the performance degradation in PSCs is mainly because of coloring in the glass substrate and the decomposition of the perovskite absorber layers. Despite the decreased PCEs, the positive outcomes in the high remaining factors in $V_{OC}$ and FF show the promise of PSCs for future space applications. Furthermore, future assessments of PSCs for space power applications should require the use of special space cover glass, space-qualified encapsulation, and more stable perovskite compositions.

## AUTHOR INFORMATION


### Corresponding Authors

*E-mail: zhaoning.song@utoledo.edu (Z.S.).
*E-mail: yanfa.yan@utoledo.edu (Y.Y.).

### ORCID

Zhaoning Song: 0000-0002-6677-0994
Woojun Yoon: 0000-0002-1946-5372
Randy J. Ellingson: 0000-0001-9520-6586
Michael J. Heben: 0000-0002-3788-3471
Yanfa Yan: 0000-0003-3977-5789


### Notes

The authors declare no competing financial interest.

## ACKNOWLEDGMENTS

This study was supported by the Office of Naval Research under contract no. N00014-17-1-2223. This material is based on the research sponsored by Air Force Research Laboratory under agreement number FA9453-18-2-0037. The U.S. Government is authorized to reproduce and distribute reprints for governmental purposes notwithstanding any copyright notation thereon. The views and conclusions contained herein are those of the authors and should not be interpreted as necessarily representing the official policies or endorsements, either expressed or implied, of Air Force Research Laboratory or the U.S. Government.

## REFERENCES


(1) Kojima, A.; Teshima, K.; Shirai, Y.; Miyasaka, T. Organometal Halide Perovskites as Visible-Light Sensitizers for Photovoltaic Cells. *J. Am. Chem. Soc.* **2009**, *131*, 6050−6051.

(2) NREL. Solar Cell Efficiency Chart. https://www.nrel.gov/pv/cell-efficiency.html (accessed July 6, 2019).

(3) Correa-Baena, J.-P.; Saliba, M.; Buonassisi, T.; Grätzel, M.; Abate, A.; Tress, W.; Hagfeldt, A. Promises and Challenges of Perovskite Solar Cells. *Science* **2017**, *358*, 739−744.

(4) Song, Z.; McElvany, C. L.; Phillips, A. B.; Celik, I.; Krantz, P. W.; Watthage, S. C.; Liyanage, G. K.; Apul, D.; Heben, M. J. A Technoeconomic Analysis of Perovskite Solar Module Manufacturing with Low-Cost Materials and Techniques. *Energy Environ. Sci.* **2017**, *10*, 1297−1305.

(5) Kaltenbrunner, M.; Adam, G.; Głowacki, E. D.; Drack, M.; Schwödiauer, R.; Leonat, L.; Apaydin, D. H.; Groiss, H.; Scharber, M. C.; White, M. S.; et al. Flexible High Power-Per-Weight Perovskite Solar Cells with Chromium Oxide-Metal Contacts for Improved Stability in Air. *Nat. Mater.* **2015**, *14*, 1032−1039.

(6) Kang, S.; Jeong, J.; Cho, S.; Yoon, Y. J.; Park, S.; Lim, S.; Kim, J. Y.; Ko, H. Ultrathin, Lightweight and Flexible Perovskite Solar Cells with an Excellent Power-Per-Weight Performance. *J. Mater. Chem. A* **2019**, *7*, 1107−1114.

(7) Yang, D.; Yang, R.; Priya, S.; Liu, S. F. Recent Advances in Flexible Perovskite Solar Cells: Fabrication and Applications. *Angew. Chem., Int. Ed.* **2019**, *58*, 4466−4483.

(8) Zhang, W.; Eperon, G. E.; Snaith, H. J. Metal Halide Perovskites for Energy Applications. *Nat. Energy* **2016**, *1*, 16048.

(9) Woodyard, J. R.; Landis, G. A. Radiation Resistance of Thin-Film Solar Cells for Space Photovoltaic Power. *Solar Cells* **1991**, *31*, 297−329.

(10) Lang, F.; Nickel, N. H.; Bundesmann, J.; Seidel, S.; Denker, A.; Albrecht, S.; Brus, V. V.; Rappich, J.; Rech, B.; Landi, G.; et al. Radiation Hardness and Self-Healing of Perovskite Solar Cells. *Adv. Mater.* **2016**, *28*, 8726−8731.

(11) Miyazawa, Y.; Ikegami, M.; Chen, H.-W.; Ohshima, T.; Imaizumi, M.; Hirose, K.; Miyasaka, T. Tolerance of Perovskite Solar Cell to High-Energy Particle Irradiations in Space Environment. *Science* **2018**, *2*, 148−155.

(12) Huang, J.; Kelzenberg, M. D.; Espinet-González, P.; Mann, C.; Walker, D.; Naqavi, A.; Vaidya, N.; Warmann, E.; Atwater, H. A. Effects of Electron and Proton Radiation on Perovskite Solar Cells for Space Solar Power Application. *2017 IEEE 44th Photovoltaic Specialist Conference (PVSC)*, June 25−30, 2017; pp 1248−1252.

(13) Miyazawa, Y.; Ikegami, M.; Miyasaka, T.; Ohshima, T.; Imaizumi, M.; Hirose, K. Evaluation of Radiation Tolerance of Perovskite Solar Cell for Use in Space. *2015 IEEE 42nd Photovoltaic Specialist Conference (PVSC)*, June 14−19, 2015; pp 1−4.

(14) Paternò, G. M.; Robbiano, V.; Santarelli, L.; Zampetti, A.; Cazzaniga, C.; Garcìa Sakai, V.; Cacialli, F. Perovskite Solar Cell Resilience to Fast Neutrons. *Sustainable Energy Fuels* **2019**, *3*, 2561−2566.

(15) Yang, S.; Xu, Z.; Xue, S.; Kandlakunta, P.; Cao, L.; Huang, J. Organohalide Lead Perovskites: More Stable Than Glass under Gamma-Ray Radiation. *Adv. Mater.* **2019**, *31*, 1805547.

(16) Yang, K.; Huang, K.; Li, X.; Zheng, S.; Hou, P.; Wang, J.; Guo, H.; Song, H.; Li, B.; Li, H.; et al. Radiation Tolerance of Perovskite Solar Cells under Gamma Ray. *Org. Electron.* **2019**, *71*, 79−84.

(17) Tu, Y.; Xu, G.; Yang, X.; Zhang, Y.; Li, Z.; Su, R.; Luo, D.; Yang, W.; Miao, Y.; Cai, R.; et al. Mixed-Cation Perovskite Solar Cells in Space. *Sci. China: Phys., Mech. Astron.* **2019**, *62*, 974221.

(18) Brus, V. V.; Lang, F.; Bundesmann, J.; Seidel, S.; Denker, A.; Rech, B.; Landi, G.; Neitzert, H. C.; Rappich, J.; Nickel, N. H. Defect Dynamics in Proton Irradiated $CH_3NH_3PbI_3$ Perovskite Solar Cells. *Adv. Electron. Mater.* **2017**, *3*, 1600438.

(19) Boldyreva, A. G.; Akbulatov, A. F.; Tsarev, S. A.; Luchkin, S. Y.; Zhidkov, I. S.; Kurmaev, E. Z.; Stevenson, K. J.; Petrov, V. G.; Troshin, P. A. γ-Ray-Induced Degradation in the Triple-Cation Perovskite Solar Cells. *J. Phys. Chem. Lett.* **2019**, *10*, 813−818.

(20) Cardinaletti, I.; Vangerven, T.; Nagels, S.; Cornelissen, R.; Schreurs, D.; Hruby, J.; Vodnik, J.; Devisscher, D.; Kesters, J.; D'Haen, J.; et al. Organic and Perovskite Solar Cells for Space Applications. *Sol. Energy Mater. Sol. Cells* **2018**, *182*, 121−127.

(21) Klein-Kedem, N.; Cahen, D.; Hodes, G. Effects of Light and Electron Beam Irradiation on Halide Perovskites and Their Solar Cells. *Acc. Chem. Res.* **2016**, *49*, 347−354.

(22) Xiao, C.; Li, Z.; Guthrey, H.; Moseley, J.; Yang, Y.; Wozny, S.; Moutinho, H.; To, B.; Berry, J. J.; Gorman, B.; et al. Mechanisms of Electron-Beam-Induced Damage in Perovskite Thin Films Revealed by Cathodoluminescence Spectroscopy. *J. Mater. Chem. C* **2015**, *119*, 26904−26911.

(23) Yuan, H.; Debroye, E.; Janssen, K.; Naiki, H.; Steuwe, C.; Lu, G.; Moris, M.; Orgiu, E.; Uji-i, H.; De Schryver, F.; et al. Degradation




DOI: 10.1021/acs.jpcc.9b11483
J. Phys. Chem. C XXXX, XXX, XXX−XXX

of Methylammonium Lead Iodide Perovskite Structures through Light and Electron Beam Driven Ion Migration. *J. Phys. Chem. Lett.* **2016**, *7*, 561−566.
(24) Kosasih, F. U.; Ducati, C. Characterising Degradation of Perovskite Solar Cells through in-Situ and Operando Electron Microscopy. *Nano Energy* **2018**, *47*, 243−256.
(25) Messenger, S. R.; Warner, J. H.; Uribe, R.; Walters, R. J. Monte Carlo Analyses of the Neo Beam Electron Beam Facility for Space Solar Cell Radiation Qualification. *IEEE Trans. Nucl. Sci.* **2010**, *57*, 3470−3476.
(26) Wang, C.; Guan, L.; Zhao, D.; Yu, Y.; Grice, C. R.; Song, Z.; Awni, R. A.; Chen, J.; Wang, J.; Zhao, X.; et al. Water Vapor Treatment of Low-Temperature Deposited $SnO_2$ Electron Selective Layers for Efficient Flexible Perovskite Solar Cells. *ACS Energy Lett.* **2017**, *2*, 2118−2124.
(27) Wang, C.; Xiao, C.; Yu, Y.; Zhao, D.; Awni, R. A.; Grice, C. R.; Ghimire, K.; Constantinou, I.; Liao, W.; Cimaroli, A. J.; et al. Understanding and Eliminating Hysteresis for Highly Efficient Planar Perovskite Solar Cells. *Adv. Energy Mater.* **2017**, *7*, 1700414.
(28) Wang, C.; Song, Z.; Yu, Y.; Zhao, D.; Awni, R. A.; Grice, C. R.; Shrestha, N.; Ellingson, R. J.; Zhao, X.; Yan, Y. Synergistic Effects of Thiocyanate Additive and Cesium Cations on Improving the Performance and Initial Illumination Stability of Efficient Perovskite Solar Cells. *Sustainable Energy Fuels* **2018**, *2*, 2435−2441.
(29) Phillips, A. B.; Song, Z.; DeWitt, J. L.; Stone, J. M.; Krantz, P. W.; Royston, J. M.; Zeller, R. M.; Mapes, M. R.; Roland, P. J.; Dorogi, M. D.; et al. High Speed, Intermediate Resolution, Large Area Laser Beam Induced Current Imaging and Laser Scribing System for Photovoltaic Devices and Modules. *Rev. Sci. Instrum.* **2016**, *87*, 093708.
(30) Wang, C.; Song, Z.; Zhao, D.; Awni, R. A.; Li, C.; Shrestha, N.; Chen, C.; Yin, X.; Li, D.; Ellingson, R. J.; et al. Improving Performance and Stability of Planar Perovskite Solar Cells through Grain Boundary Passivation with Block Copolymers. *Solar RRL* **2019**, *3*, 1900078.
(31) Chen, B.; Yang, M.; Priya, S.; Zhu, K. Origin of J-V Hysteresis in Perovskite Solar Cells. *J. Phys. Chem. Lett.* **2016**, *7*, 905−917.
(32) Abate, A.; Leijtens, T.; Pathak, S.; Teuscher, J.; Avolio, R.; Errico, M. E.; Kirkpatrik, J.; Ball, J. M.; Docampo, P.; McPherson, I.; et al. Lithium salts as "redox active" p-type dopants for organic semiconductors and their impact in solid-state dye-sensitized solar cells. *Phys. Chem. Chem. Phys.* **2013**, *15*, 2572−2579.
(33) Čermák, J.; Mihai, L.; Sporea, D.; Galagan, Y.; Fait, J.; Artemenko, A.; Štenclová, P.; Rezek, B.; Straticiuc, M.; Burducea, I. Proton Irradiation Induced Changes in Glass and Polyethylene Terephthalate Substrates for Photovoltaic Solar Cells. *Sol. Energy Mater. Sol. Cells* **2018**, *186*, 284−290.
(34) Gusarov, A. I.; Doyle, D.; Hermanne, A.; Berghmans, F.; Fruit, M.; Ulbrich, G.; Blondel, M. Refractive-index changes caused by proton radiation in silicate optical glasses. *Appl. Opt.* **2002**, *41*, 678−684.
(35) Song, Z.; Abate, A.; Watthage, S. C.; Liyanage, G. K.; Phillips, A. B.; Steiner, U.; Graetzel, M.; Heben, M. J. Perovskite Solar Cell Stability in Humid Air: Partially Reversible Phase Transitions in the $PbI_2$-$CH_3NH_3I$-$H_2O$ System. *Adv. Energy Mater.* **2016**, *6*, 1600846.
(36) Huang, J.; Tan, S.; Lund, P. D.; Zhou, H. Impact of H2o on Organic-Inorganic Hybrid Perovskite Solar Cells. *Energy Environ. Sci.* **2017**, *10*, 2284−2311.
(37) Juarez-Perez, E. J.; Ono, L. K.; Maeda, M.; Jiang, Y.; Hawash, Z.; Qi, Y. Photodecomposition and Thermal Decomposition in Methylammonium Halide Lead Perovskites and Inferred Design Principles to Increase Photovoltaic Device Stability. *J. Mater. Chem. A* **2018**, *6*, 9604−9612.
(38) Divitini, G.; Cacovich, S.; Matteocci, F.; Cinà, L.; Di Carlo, A.; Ducati, C. In Situ Observation of Heat-Induced Degradation of Perovskite Solar Cells. *Nat. Energy* **2016**, *1*, 15012.
(39) Song, Z.; Wang, C.; Phillips, A. B.; Grice, C. R.; Zhao, D.; Yu, Y.; Chen, C.; Li, C.; Yin, X.; Ellingson, R. J.; et al. Probing the Origins of Photodegradation in Organic-Inorganic Metal Halide Perovskites with Time-Resolved Mass Spectrometry. *Sustainable Energy Fuels* **2018**, *2*, 2460−2467.
(40) Bae, S.; Kim, S.; Lee, S.-W.; Cho, K. J.; Park, S.; Lee, S.; Kang, Y.; Lee, H.-S.; Kim, D. Electric-Field-Induced Degradation of Methylammonium Lead Iodide Perovskite Solar Cells. *J. Phys. Chem. Lett.* **2016**, *7*, 3091−3096.
(41) Zhou, Y.; Zhao, Y. Chemical Stability and Instability of Inorganic Halide Perovskites. *Energy Environ. Sci.* **2019**, *12*, 1495−1511.
(42) Tai, Q.; Tang, K.-C.; Yan, F. Recent Progress of Inorganic Perovskite Solar Cells. *Energy Environ. Sci.* **2019**, *12*, 2375−2405.
(43) Jung, E. H.; Jeon, N. J.; Park, E. Y.; Moon, C. S.; Shin, T. J.; Yang, T.-Y.; Noh, J. H.; Seo, J. Efficient, Stable and Scalable Perovskite Solar Cells Using Poly(3-Hexylthiophene). *Nature* **2019**, *567*, 511−515.
(44) Wang, Y.; Dar, M. I.; Ono, L. K.; Zhang, T.; Kan, M.; Li, Y.; Zhang, L.; Wang, X.; Yang, Y.; Gao, X.; et al. Thermodynamically Stabilized $\beta$-$CsPbI_3$−Based Perovskite Solar Cells with Efficiencies >18%. *Science* **2019**, *365*, 591−595.


DOI: 10.1021/acs.jpcc.9b11483
J. Phys. Chem. C XXXX, XXX, XXX−XXX